Chapter 2:

METHODOLOGY

Chapter 2:
Methodology

2.1. Seismic Data Acquisition and Processing

The Seismological data used in the present study was acquired with the help of broadband seismographs installed by Wadia Institute of Himalayan Geology (WIHG), Dehradun in the NW Himalaya region. These seismographs were equipped with Trillium- 240 broadband sensors. These sensors were used to record the earthquake data at 100 samples. These sensors were also attached with a 24-bit Taurus digitizer. A GPS was also attached along with the digitizer so that the timing system could be synchronised with higher accuracy. The seismic data used in this study was recorded during 2004 to 2013. The recorded earthquake waveforms were analysed for earthquake hypocenter locations using the SEISAN software (Havskov and Ottemueller, 1999), which utilizes the HYPO71 program (Lee and Lahr, 1975) for earthquake locations. The earthquake data acquired with the help of seismometer was recorded and extracted in SEED format with the help of RDSEED program encoded inside the Seisan software. Next this earthquake data was merged according to their arrival times and registered with an assigned database. Then the database was registered with the WAV and REA sub directory using the command MAKEREA.*Figure 2.1* represents the command window showing an example for the sub directories created with the MAKEREA and MAKEWAV command in the Command prompt.

Figure 2.1: The command window showing an example for the sub directories created with the MAKEREA and MAKEWAV command.

Following the database created inside the WAV and REA sub-directories, merged events with the WAV directory were acquired. Next the waveform data was registered with the database and the all the information related with its arrival times are registered with the REA sub-directory. The database registered with the REA directory assigned the waveform data according to its arrival year and month. After registering the event with the database it was plotted using the command EEV. The recorded waveform data comsists of three components of digital seismograms. These threee components may be termed as Z or vertical component; N or north-south

component and E or east-west component. In this way the earthquake data were plotted and arrival times are picked and earhquake data was located using minimum of six components recorded with these three stations.*Figure 2.2* shows the example seismic waveform window for the earthquake of 09.07.2013 earthquake event of magnitude (Mw = 5.1) recorded at the WIHG seismic stations operated in NW Himalaya.

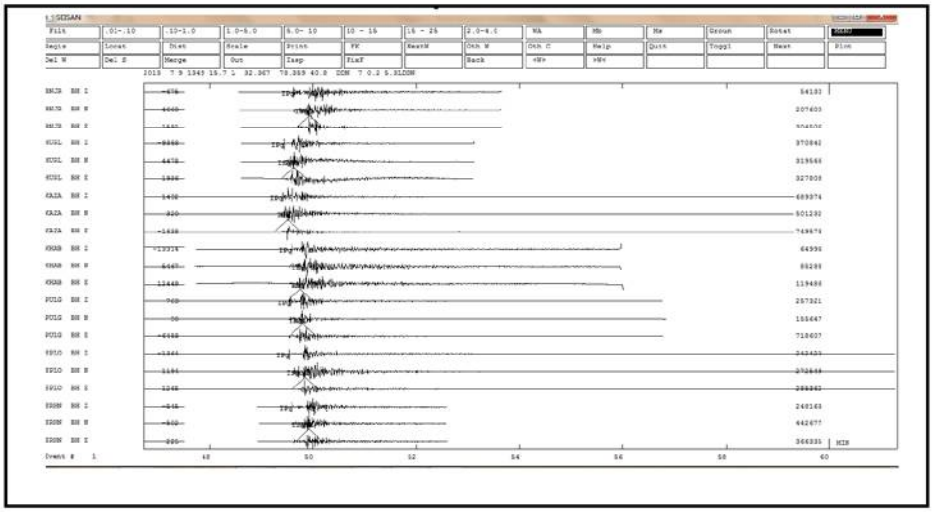

Figure 2.2: The example seismic window shown for the earthquake of 09.07.2013 earthquake event of magnitude (Mw = 5.1) recorded at the WIHG seismic stations operated in NW Himalaya.

The earthquake events were processed and located with the HYPO71 location software (Lee and Lahr., 1975) encoded in the Seisan software. It uses the standard alogorithm and the location of the recording stations along with its elevation. The location parameters mainly contains the latitude , longitude, depth, magnitude, root mean square (RMS) error calculated for the event located from arrival time information. *Figure 2.3* demarcates the command window showing the arrival times of earthquake at different recording seismic stations for the earthquake of 09.07.2013 earthquake event of magnitude (Mw = 5.1) recorded at the WIHG seismic stations operated in NW Himalaya.

For location, the standard velocity model available for the NW Himalaya as proposed by Kumar et al., 2009 has been used.

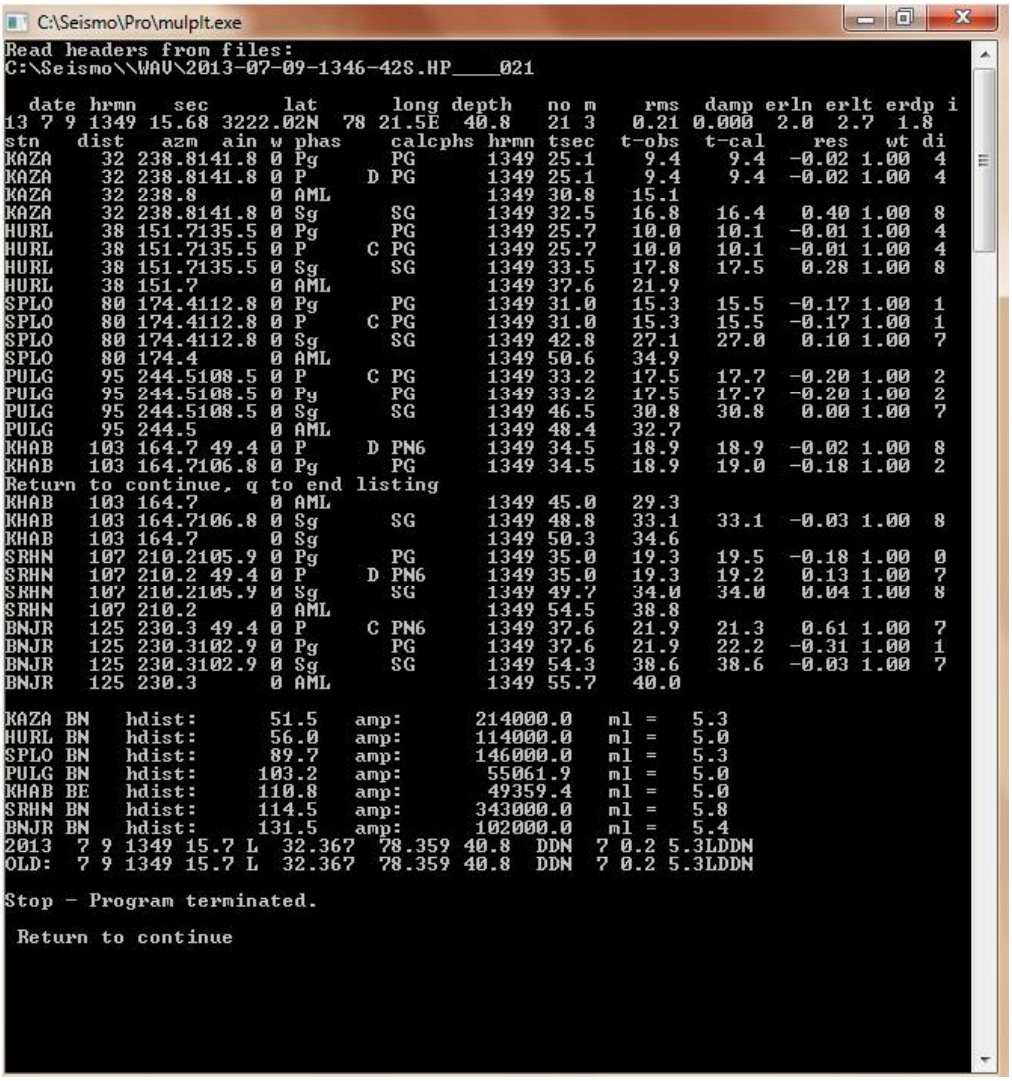

Figure 2.3: The command window showing the arrival times of earthquake at different recording seismic stations for the earthquake of 09.07.2013 earthquake event of magnitude (Mw = 5.1) recorded at the WIHG seismic stations operated in NW Himalaya.

2.2. Determining the 1 D Crustal Velocity Model

The structure and composition of the earth can be identified along with the accurate hypocentral location parameters with the knowledge from the velocity structure of that region. The method used for calculating the velocity structureusing the inversion of arrival times of the earthquake events at the recording stations is theinbuilt VELEST package (Kissling. et al., 1994) inside the Seisan software, (Havskov and Ottemoller, 1999). This method utilizes the

least square technique as described in detail in Crosson (1976). The technique computes the travel times from the earthquakes to the arrival seismic stations by assuming a non-linear travel time function that shows its dependency on velocity parameters, hypocenter parameters and the station corrections. This program for determining the 1 D minimum velocity model was first framed under the name HYPO2D D (Ellsworth 1977; Roecker, 1981). The detailed description regarding the minimal 1 D velocity model derivation can described as follows. First of all minimum 1 D velocity modeldetermined with the VELEST algorithm before relocating the earthquake hypocenters with higher degree of accuracy in terms of origin time, latitude, longitude and depth. The first step followed before computing the minimum 1 D crustal velocity model involves acquiring all the priori information regarding the velocities and the layer thickness etc. for the study area. This can be obtained from previously determined velocity models for the particular region. A maximum set of 500 best earthquake events with a high quality P and S-wave arrival times were recorded with in the network were selected. Then these earthquake events were simultaneously inverted along with the priori velocity model with a damping coefficient of 0.01 for hypocentral parameters and 0.1 for velocity model parameters. Next, theinversion for hypocenters, station delays and velocity model parameters is repeated with updated new velocity models in the priori velocity model along with new station delays and new hypocenter locations till it will reach a minimal squared error associated with the locations. Here for the derivation can be of the minimum 1 D velocity model,the model proposed by Kumar et al., 2009 using the steps described in flowchart below (*Figure 2.4*), have been utilized, which is a five layered velocity model with a maximum estimated depth of around 46 km. The minimum 1 D velocity model obtained in the present study has been discussed in detail in the next chapter i.e. chapter 3. The detailed model is a seven layer velocity model with low rms error and high efficiency in earthquake location.*Figure 2.4* represents the flow chart describing the running procedure for the VELEST program by following the above mentioned procedure the minimum 1 D crustal velocity model has been determined for the NW Himalaya region.*Figure 2.5* shows the command window describing the

program VELMENU operation while computing the minimum 1 D crustal velocity model .

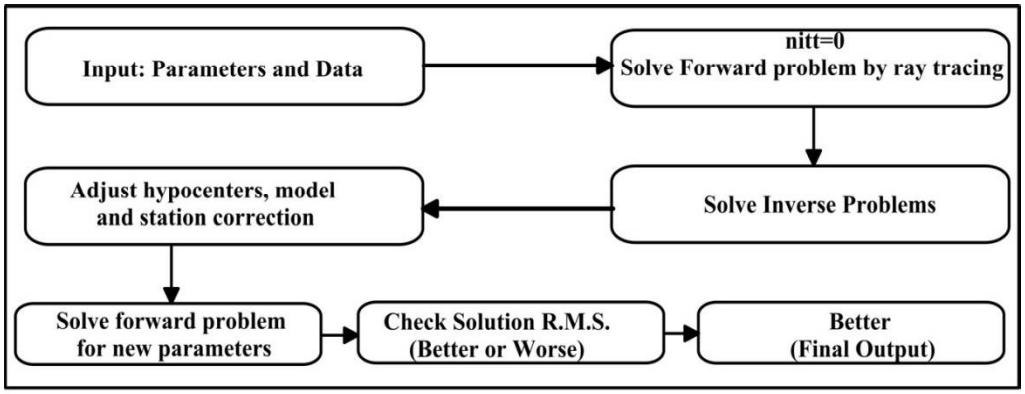

Figure 2.4: The flow chart describing the running procedure for the VELEST program by following the above mentioned procedure the minimum 1 D crustal velocity model has been determined for the NW Himalaya region.

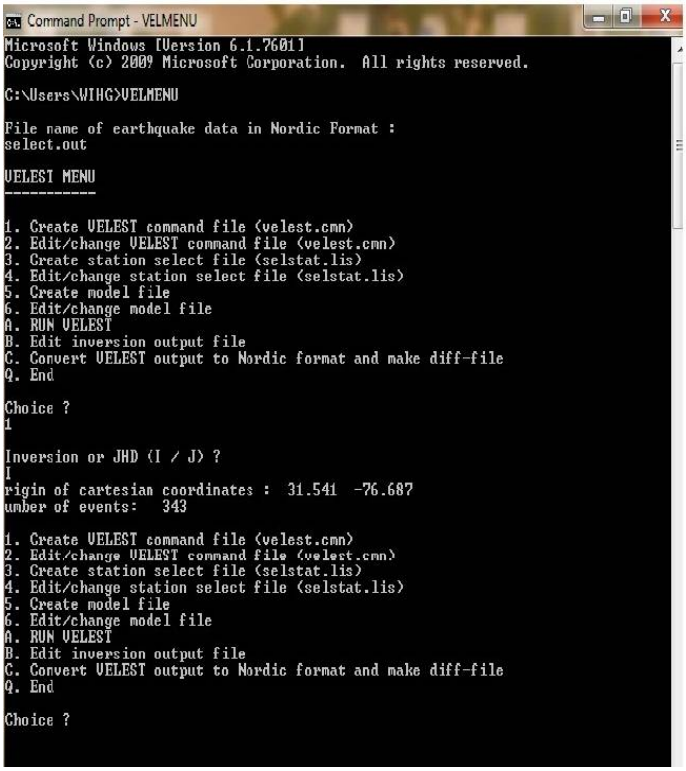

Figure 2.5: The command window describes the program VELMENU operation while computing the minimum 1 D crustal velocity model .

2.3. Double-difference Relocation of Seismicity using HypoDD

Relocation of earthquake hypocenters in the study region is achieved utilizing the HypoDD, double-difference program of Waldhauser and Ellsworth (2000). The double difference algorithm has been derived by applying the first degree tailor series expansion to the earthquake location equation given by Geiger (1912). The relocation of earthquake events is achieved when the fact of small hypocentral separation between the pair of earthquake events exists as compared to its distance from both the common recorded receiver station. Accordingly, a set of differential travel time pairs for the earthquakes at common stations are determined by utilizing a one dimensional velocity model having its variation only with respect to depth. There are certain discrepancies in earthquake location due to the uncertainties resulting from non-availability of correct velocity model, bad receiving station geometry, wrong reading of the arrival times at the stations (Pavlis, 1986; Gomberg et al., 1990) etc. Again with this method the minimum residuals corresponding to hypocentral parameters that are unknown (Origin time, latitude, longitude and depth) are obtained utilizing either the method of conjugate gradients method (LSQR, Paige and Saunders, 1982) or the singular value decomposition (SVD) method. In the present work, the conjugate gradient methods have been applied for our hypocenter relocation in the study region. The input for earthquake relocation can be prepared utilizing the data consisting of the arrival time information from different earthquake catalogues and can be termed as catalog data as used in the present analysis. Moreover, the cross correlation data obtained using the differential arrival time pairs from phase correlation of P- and/or S-waves. The HypoDD program utilized in the current seismicity relocation has been worked with two sub phases. The first one comprising of the preparation of differential arrival time pairs for earthquake hypocenters and this has been achieved utilizing the "*Ph2dt*"subroutine program of the HypoDD algorithm. This program also needs some inputs before preparing the differential arrival time pairs. These inputs are predefined under various category such as MAXSEP, MAXNGH, MINLNK, MAXDIST, MINWGT, MINOBS and MAXOBS. "*Ph2dt*"program works on the basis of the provided inputs under the above mentioned

categories. The MAXSEP signifies the maximum separation between the events pairs defined within the search radius. The links between neighbouring events pairs are determined on the basis of number of neighbouring event pairs greater than the MINLINK phase pairs. This link between individual hypocenters to maximum hypocenters is established using the MAXNGH option. The maximum search radius is defined on the basis of the input provided under the MAXDIST option. The values under MINOBS and MAXOBS depends on the total number of hypocenters used for the study utilizing a larger number of events, then it need only strongly connected hypocenters so that it can be provided with same value for MINOBS as to MINLINK. On the other hand a small data set is utilized, MINOBS = 1, MAXOBS to the number of stations, and MAXNGH to the number of events must be utilized. The inputs for the program "*ph2dt*"under various categories as mentioned above and prepared the differential arrival time pairs for relocating it further with the HypoDD program. The outputs derived from "*ph2dt*"are placed under the files "*dt.ct*" containing the differential arrival time pairs, "*event.dat*" file containing the event information and the "*station.dat*" containing the station information. After attainment of these inputs, the input file named "*hypoDD. inp*" is edited for type of data i.e. catalog data as used for this study, for different arrival times of P and S Phase, the maximum distance of the hypocenters, the type of solution control method, the weighting scheme for both P and S phases respectively. After providing the particular values under these sub-classes of the program the program HypoDD is set to run and two output files containing the location and relocation of earthquake hypocenters are obtained. These two files are termed as the final outputs of this double-difference earthquake relocation programs.

2.4. Determination of Focal mechanisms

To understand the physical motion associated with the faults one should have the knowledge about the source parameters. To understand this, the information with higher accuracy about the hypocentral parameters and seismic moment is needed. This is achieved through analysing the entire seismogram observed and recorded at the receiver seismic station. There are a

number of waveform inversion methods proposed in past for getting the information on source parameters along with the hypocentral parameters. A few may be named as the codes given by Dreger and Helmberger, 1993; Kikuchi and Kanamori, 1991; McCaffrey et al., 1991 that can be extensively used for inverting teleseismic waveforms. For inverting regional waveforms, these codes are widely applicable however these codes limits accuracy and high computational speed as compared to the present code ISOLA given by Zahradnik et al. (2005) have been utilized. Therefore, in the present study, the ISOLA code given by Zahradnik et al. (2005) is applied for determining the moment tensors for local as well as regional earthquakes recorded with the broad band sensors deployed in the NW Himalaya. The working principle governing this code can be described in detail as follows-:

This program is based on the multiple point-source representation and iterative deconvolution method, similar to Kikuchi and Kanamori (1991) for teleseismic records. In the present study, the full wave field is considered, and Green's functions are calculated by the discrete wavenumber method of Bouchon (1981). This program utilizes the FORTRAN processing language for fast computation speed and MATLAB platform for good graphical images. It is well known that determination of the source characteristics is not a linear approach and it has to be solved iteratively for the parameters through nonlinear inversion. Thus before proceeding to have a good real-synthetic match with the code there should be a proper selection of seismogram windows with appropriate frequency bands should be worked with. The interactive graphical mode provides an advantage for simultaneous real-synthetic match of the seismic waveforms along with solving non-uniqueness of the inversion.The complete seismogram of earthquake is first converted to *SAC* format for all the three components and again from these formats it is further converted to the *ASCII* format using Matlab codes (*m-files*) freely available on the Web6 (Thorne, 2005). Then the instrument correction is applied utilizing the pole and zero files by applying proper frequency range as the whole data may contain high frequency noise that can affect the inversion, while at the same time these are not easily recognizable in the time series data (Zahradnik and Plesinger, 2005). After applying all the procedures mentioned

above, the waveform inversion is carried out in the following steps. *Figure 2.6* shows the graphic user interface (GUI) for the ISOLA program utilized for determining the moment tensor focal mechanisms for the local and regional seismic waveforms.

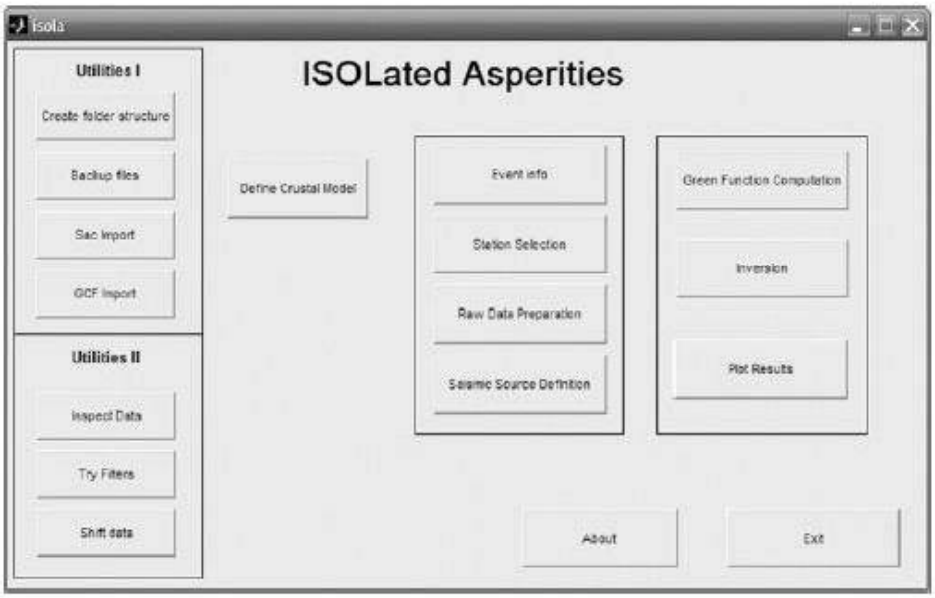

Figure 2.6: It shows the graphic user interface (GUI) for the ISOLA program utilized for determining the moment tensor focal mechanisms for the local and regional seismic waveforms.

The first part is the preparation of a crustal velocity model utilizing the *crustmod* tool. Here, seven layers P-wave and S-wave velocity model have been applied for the analysis. The other parameters such as density quality factors for both P-wave and S-wave designated as ρ expressed in g/cc, Q_p *and* Q_s are also estimated using the available empirical relations in the code. Only single crustal model as the velocity model in the analysis have been used. *Figure 2.7* shows the graphic user interface (GUI) for the ISOLA program showing the utilized 1 D crustal velocity model for determining the moment tensor.

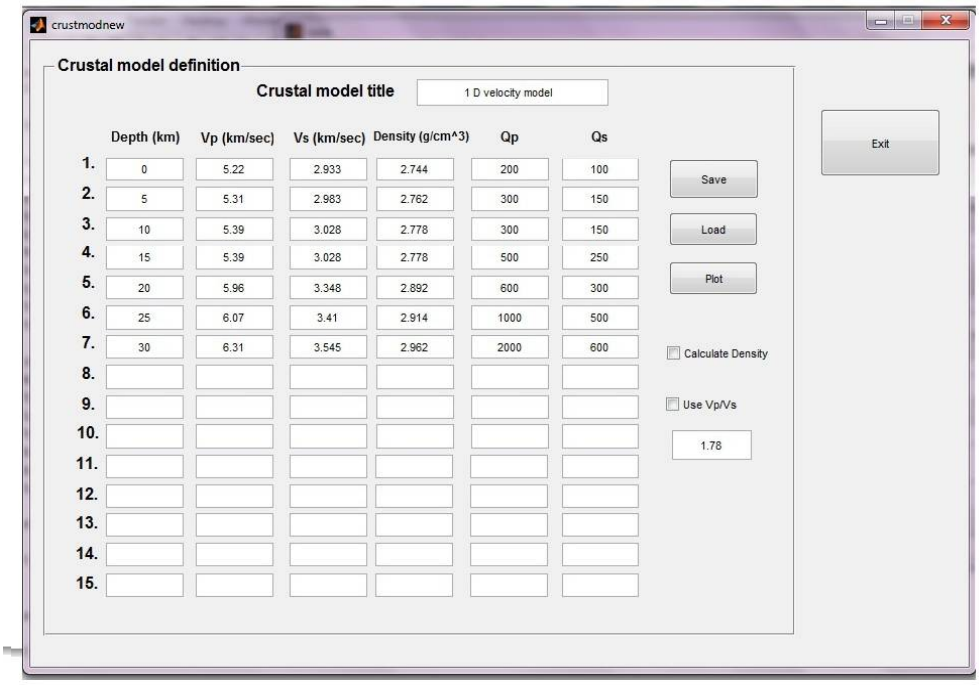

Figure 2.7: Figure signifies the graphic user interface (GUI) for the ISOLA program showing the utilized 1 D crustal velocity model for determining the moment tensor.

In the next step, earthquake information is provided which includes the date of the earthquake event, origin time, latitude, longitude and depth as calculated from earthquake location using the *eventinfo* tool. The time window in seconds that is to be utilized for inversion is also provided here with the application of the *eventinfo* tool. Figure 2.8 designates the window of the graphic user interface (GUI) for the ISOLA program showing the earthquake event details (date, Latitude, Longitude Depth, origin time, magnitude, time window length) reported by the United State Geological Services (USGS) studied for determining the moment tensor.

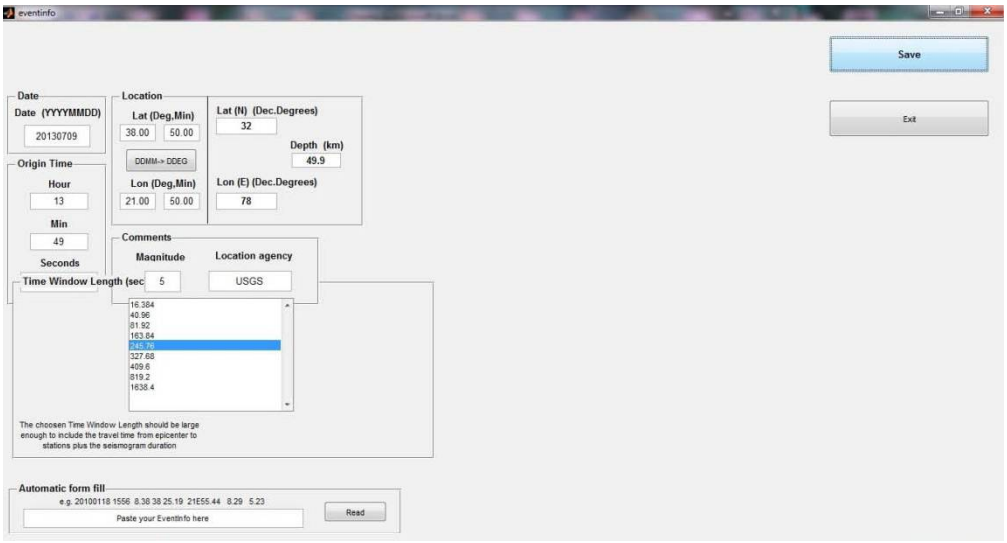

Figure 2.8: This window presents the graphic user interface (GUI) for the ISOLA program showing the earthquake event details (date, Latitude, Longitude Depth, origin time, magnitude, time window length) reported by the United State Geological Services (USGS) studied for determining the moment tensor.

In the next step the seismological stations whose waveform data needs to be inverted are selected utilizing the *stationselect* tool. Then the *m_Map* program of Matlab encoded within the ISOLA program is used for this purpose. *Figure 2.9* shows the window of the graphic user interface (GUI) for the ISOLA program showing the earthquake event and the selected recording seismic stations utilized for moment tensor inversion.

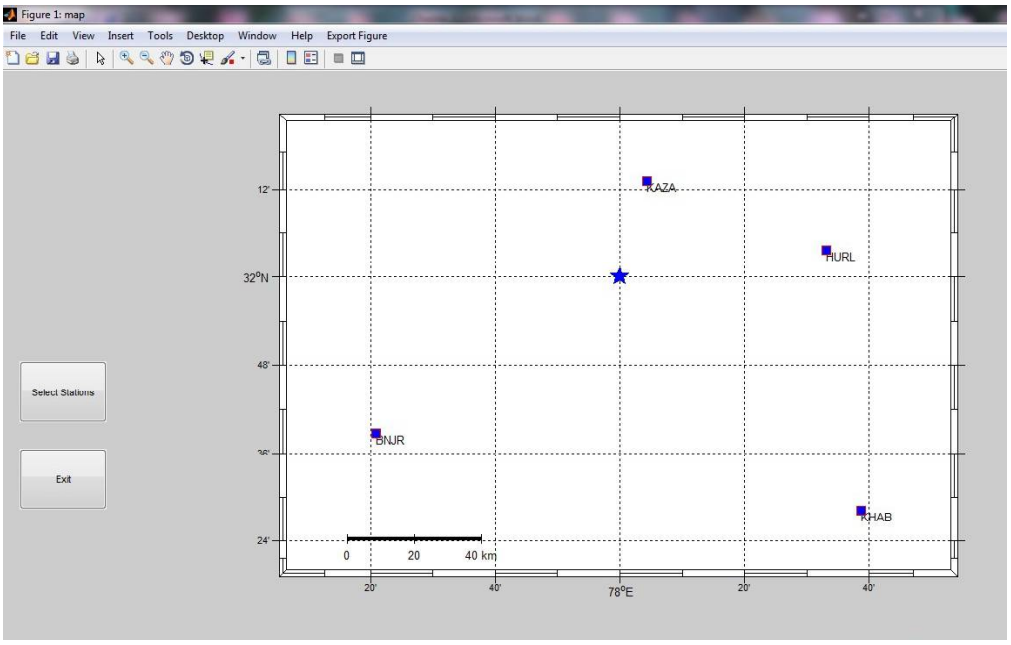

Figure 2.9: This window presents the graphic user interface (GUI) for the ISOLA program showing the earthquake event and the selected recording seismic stations utilized for moment tensor inversion.

Next, data for inversion of all the seismic stations used for the study is prepared utilzing the data preparation tool encoded within the Isola program. Within this sub routine program data is imported and baseline correction, instrument correction, origin time allignment etc. is carried out within appropriate frequency band. The data is finally saved in appropriate format after applying all the corrections.*Figure 2.10* represents the window of the graphic user interface (GUI) for the ISOLA program showing the seismic waveform after applying the instrument corrections at a selected recording seismic stations utilized for moment tensor inversion.

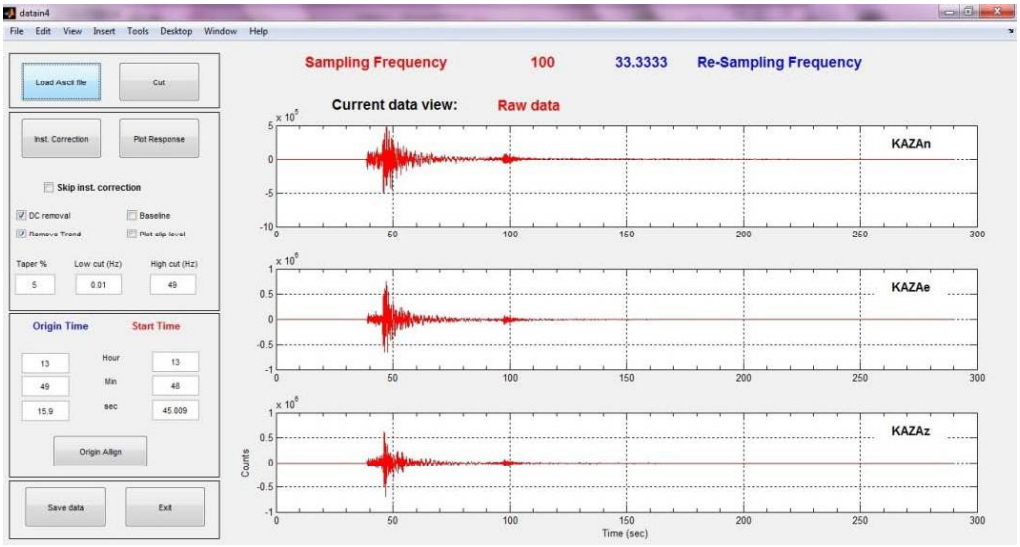

Figure 2.10: This window presents the graphic user interface (GUI) for the ISOLA program showing the seismic waveform after applying the instrument corrections at a selected recording seismic stations utilized for moment tensor inversion.

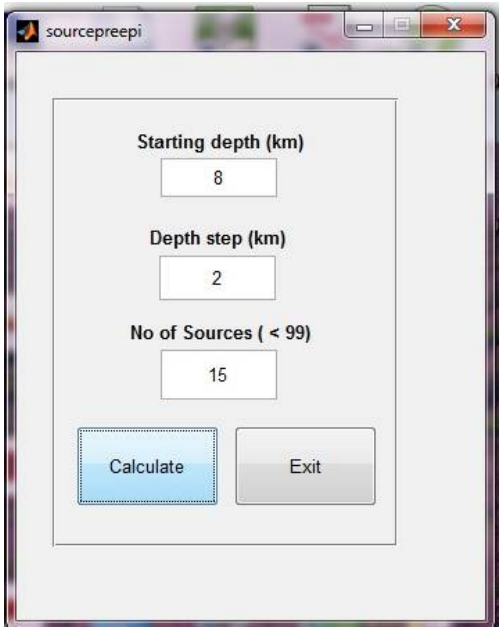

Figure 2.11: This window presents the graphic user interface (GUI) for the ISOLA program showing the starting depth for source or earthquake hypocenter and each depth step for source inversion along with the maximum number of sources to be utilized for source depth.

After assigning the proper crustal velocity model within the GUI (Graphical user interface) along with other input preparations options like data pre-processing, source preparation, Greens function generation and final step inversion are carried out step wise. The data is saved in proper format after applying the instrument correction and selecting the seismogram with good signal to noise ratio. The output files are then stored in the particular directories and used when required. Then the particular source position is assigned through *sourcepre* tool and at each depth with definite depth spacing is searched up to the maximum source depth and here it is assigned upto 50 km. Two options for assigning the particular source type are available: the first one is the "*Point*" which specifies the presence of source below the epicenter and the "*Extended*" one that specifies a particular plane at a certain depth with a depth range with an arbitrary orientation. In this way the inversion will find the optimum position of the event in space. The program generates all necessary input files in the following step required for computation of Green's function and inversion that have to be carried out in the next steps. Here for eg. a starting depth of 8 km below the epicenter is given. The depth step for computing the Green's function is also given and the total number of sources required for the generation is also given as an input in the following step.*Figure 2.11* shows the window of the graphic user interface (GUI) for the ISOLA program showing the starting depth for source or earthquake hypocenter and each depth step for source inversion along with the maximum number of sources to be utilized for source depth.

In the next step Green's functions are computed using the frequency wavenumber method (Bouchon, 1981). Green's functions are nothing but it specifies the response of the earth to the seismic waves at particular frequencies. The Green's functions are generated utilizing the *greenpre* tool of ISOLA program. The program generates the synthetic seismograms at specified maximum frequency and stores in particular sub directories. *Figure 2.12* presents the window of the graphic user interface (GUI) for the ISOLA program showing the Greens function computation for each earthquake source at different source depths.

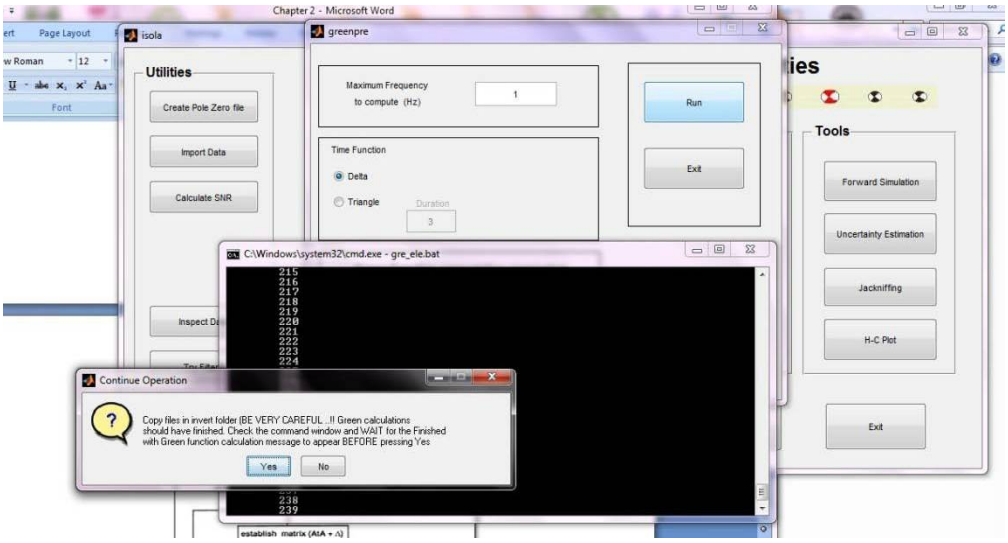

Figure 2.12: This window presents the graphic user interface (GUI) for the ISOLA program showing the Greens function computation for each earthquake source at different source depths.

The most important and last step of this work is to perform the inversion procedure discussed above and the matching of the observed and the synthetic seismogram. This inversion is performed utilizing the invert tool. Under this program, one needs to specify the particular frequency band for performing the inversion. The performer needs to specify which kinds of inversion have to perform, for e.g. full, deviatoric, double couple (DC) as well as the number of subevents, and time span of their occurrence. *Figure 2.13* presents the window of the graphic user interface (GUI) for the ISOLA program showing the Inversion routine for a single earthquake event at a particular frequency band. Other options like assigning the weights to seismogram at particular seismic stations, correlation and focal mechanism *vs.* source position and its time shift, double couple percentage of the solution (DC%) can also be plotted, since in many cases it can provide indication about problematic inversion results.

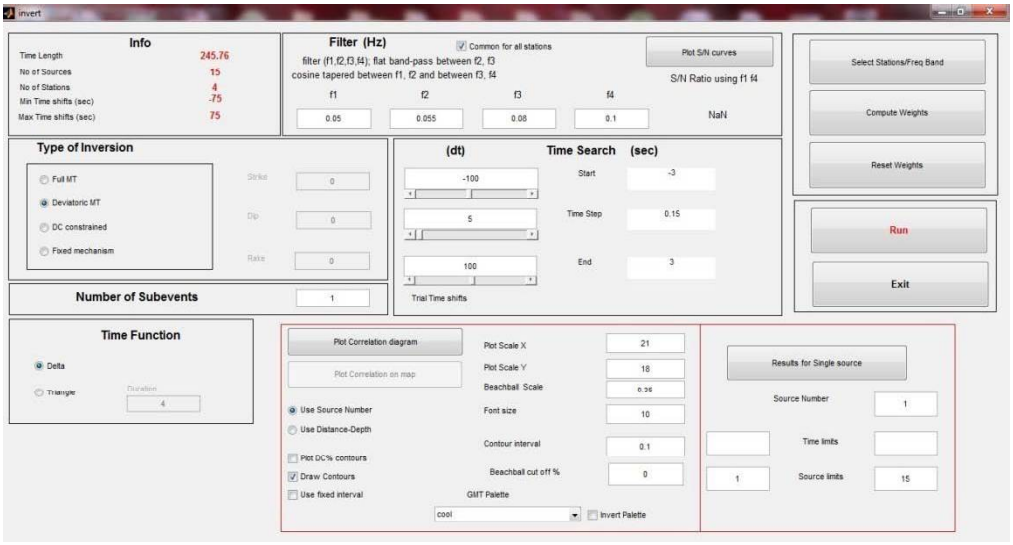

Figure 2.13: This window presents the graphic user interface (GUI) for the ISOLA program showing the Inversion routine for a single earthquake event at a particular frequency band.

The outputs generated utilizing the Isola inversion sub routine program consists of mainly the real-synthetic match, the type of solution and its correlation with the source depth, percentage of Double couple (DC%) and its relationship with the correlation obtained from grid search method and source position and time. Therefore this technique for determination of focal mechanism solutions to dignify the tectonic kinematics of the study area, ISOLA code is utilized and results are achieved. The following outputs are given in pictorial form below. *Figure 2.14* shows the window presenting the graphic user interface (GUI) for the ISOLA program showing the real synthetic match for the seismic event after carrying out the Inversion routine program for a particular frequency band. *Figure 2.15* shows the window presenting the graphic user interface (GUI) for the ISOLA program showing the maximum correlation obtained for the focal mechanism solution at different source depths and the Double-Couple is expressed in percentage scale as DC% for the seismic event after carrying out the Inversion routine program for a particular frequency band. *Figure 2.16* shows the window presenting the graphic user interface (GUI) for the ISOLA program showing the maximum correlation plotted as a function of Double-Couple expressed in percentage scale as DC% with the

different grid searches for the seismic event after carrying out the Inversion routine program for a particular frequency band. *Figure 2.17* represents the window of the graphic user interface (GUI) for the ISOLA program showing the maximum correlation plotted as a function of source position and source time for the seismic event after carrying out the Inversion routine program for a particular frequency band.

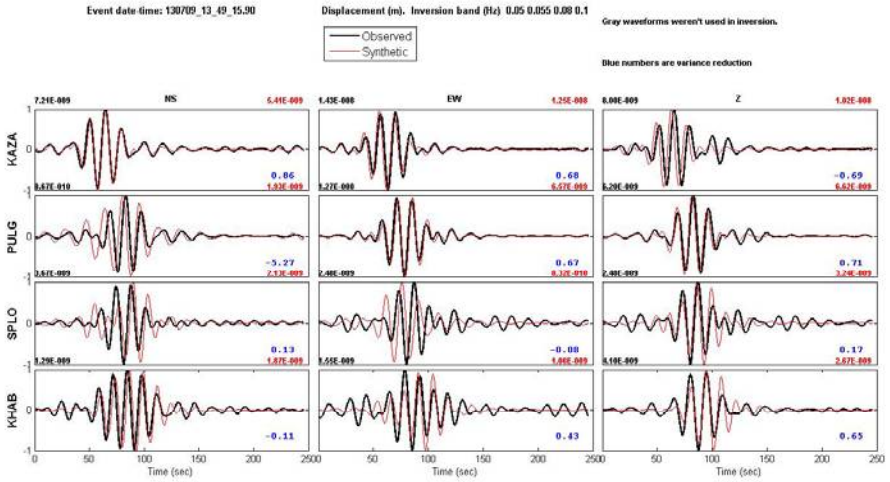

Figure 2.14: This window presents the graphic user interface (GUI) for the ISOLA program showing the real synthetic match for the seismic event after carrying out the Inversion routine program for a particular frequency band.

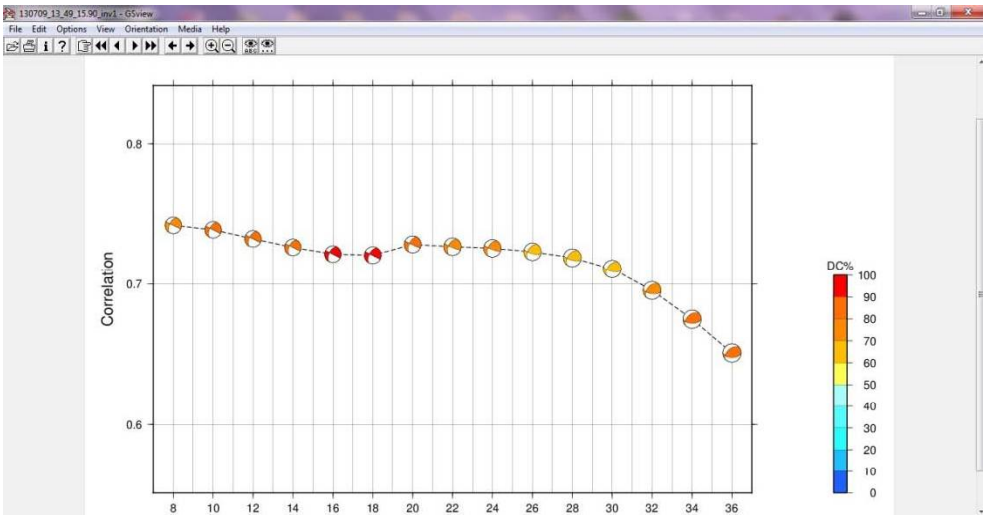

Figure 2.15: This window presents the graphic user interface (GUI) for the

ISOLA program showing the maximum correlation obtained for the focal mechanism solution at different source depths and the Double-Couple is expressed in percentage scale as DC% for the seismic event after carrying out the Inversion routine program for a particular frequency band.

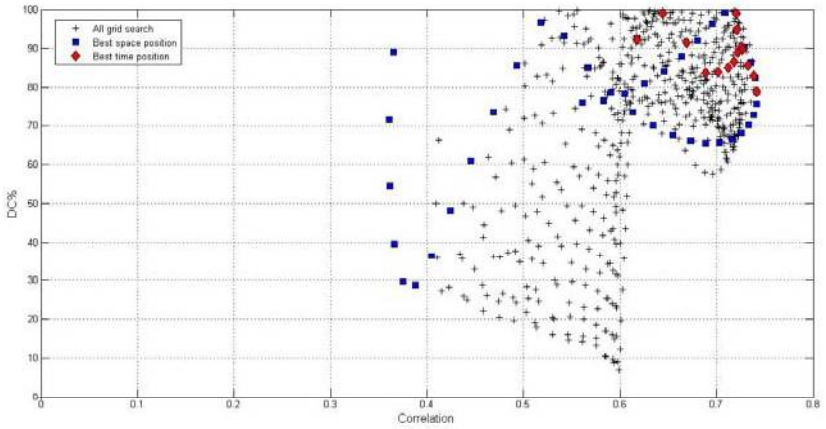

Figure 2.16: This window presents the graphic user interface (GUI) for the ISOLA program showing the maximum correlation plotted as a function of Double-Couple expressed in percentage scale as DC% with the different grid searches for the seismic event after carrying out the Inversion routine program for a particular frequency band.

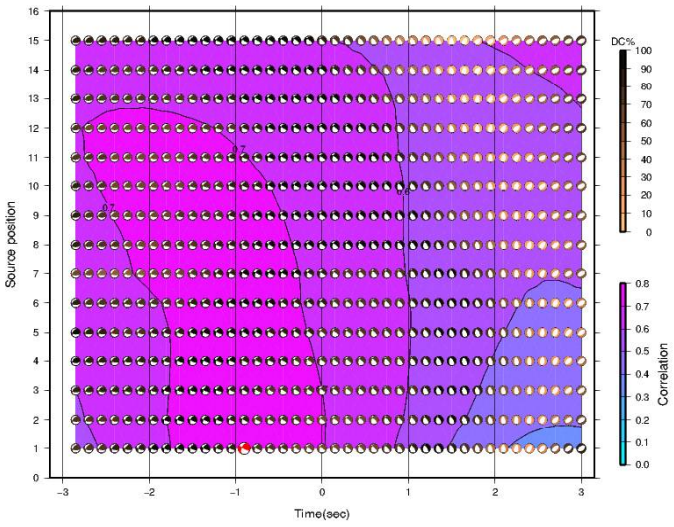

Figure 2.17: This window presents the graphic user interface (GUI) for the

ISOLA program showing the maximum correlation plotted as a function of source position and source time for the seismic event after carrying out the Inversion routine program for a particular frequency band.

2.5. Estimation of Static Stress Transfer Phenomenon in NW Himalaya

The static stress change due to the three major earthquakes namely the 1905 Kangra earthquake, 1975 Kinnaur earthquake, 1991 Uttarkashi earthquake and 1999 Chamoli earthquake that occurred in NW Himalaya, India were studied utilizing the Coulomb 3.1 application (Stein, 1999). This application is based on the equation that shows the change in the static stress change (ΔCFS) on a specified fault due to an earthquake and can be described below as:

$$\Delta CFS = \Delta\tau - \mu' (\Delta\sigma n) \qquad (2.1)$$

where $\Delta\tau$ is the change in shear stress calculated on the orientation and kinematics of either optimally oriented faults, or specified faults, μ' is the coefficient of effective friction, and $\Delta\sigma n$ is the change in normal stress. According to this failure occurs due to the change in static stress on the receiver faults due to the occurrence of earthquake on source fault. Source faults can be described as the faults that have slip, and so they impart stress to the surrounding crust and faults. Again Receiver Faults (almost always) are those who receives the imparted stress from the source fault and generally have no slip. The program is used here in the study for estimating the stress transfer phenomenon in the NW Himalaya due to the occurrence of major earthquakes in the region. This program also requires some inputs before computing the static stress change on receiver or targeted faults due to the present tectonic convergence. This program also uses the MATLAB platform for computation of static stress changes. This also uses a Graphic user interface (GUI) for its computation. The Coulomb calculations require input files; some require successive information for which every time the user is prompted for. Here the input is prepared for estimating the coulomb stress in appropriate format. The input files can be prepared in two appropriate formats

namely the *(.inp*) format which specifies the source slip by right-lateral and reverse slip (left lateral or normal slip are negative) and the other one is an alternate *(.inr*) input format that specifies rake (°) and netslip, which permits one to calculate the stress change on receivers (faults without slip) in their rake directions, where, for example, a left-lat. stress increase would inhibit failure on a right-lateral fault. Therefore for preparing the input file in (.inr) format one had to first open the Input option and then choose *Input > Open & edit input file >*. Here in the present analysis the input file built in (.inr) format is shown below.*Figure 2.18* shows the window presenting the graphic user interface (GUI) for the Coulomb 3.1 application showing the inputs incorporated required for computing the static stress imparted on the receiver fault due to the earthquake.

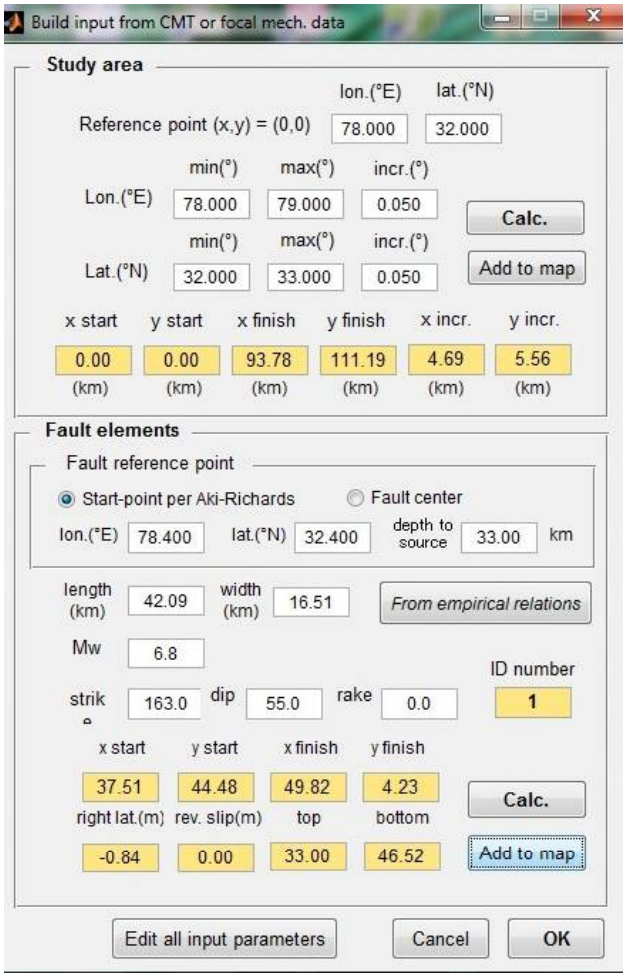

Figure 2.18: This window presents the graphic user interface (GUI) for the

Coulomb 3.1 application showing the inputs incorporated required for computing the static stress imparted on the receiver fault due to the earthquake.

In this study, base map in latitude and longitude format. For preparing the input we need to have the location of the source fault or the earthquake source location, the strike, dip and rake of the source fault, the moment magnitude (Mw) for the earthquake source and the depth of the source point. The length and width of the source fault or earthquake rupture parameters are deduced by utilizing the empirical relationship given by Wells and Coppersmith, 1994. *Figure 2.19* figure represents the graphic user interface (GUI) for the Coulomb 3.1 application showing the source fault is shown in the region.

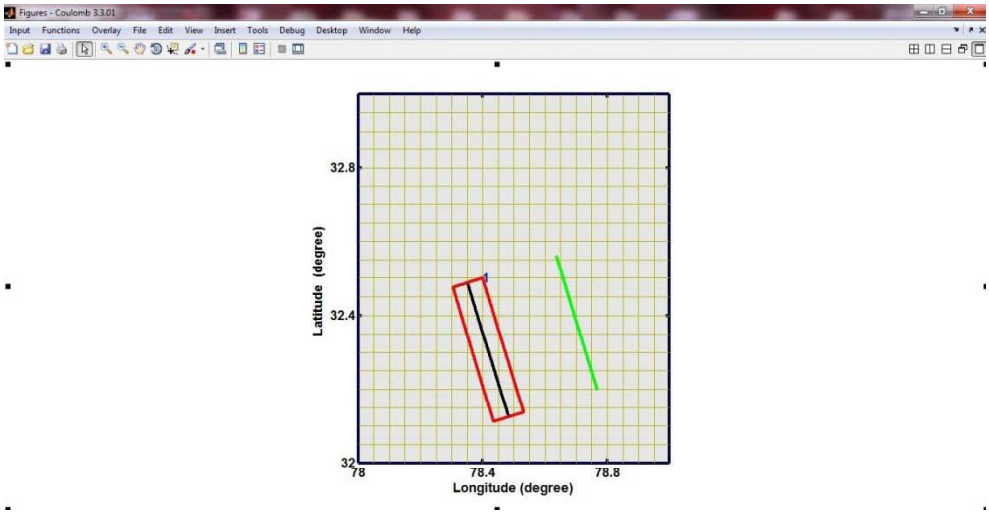

Figure 2.19: The above figure represents the graphic user interface (GUI) for the Coulomb 3.1 application showing the source fault is shown in the region.

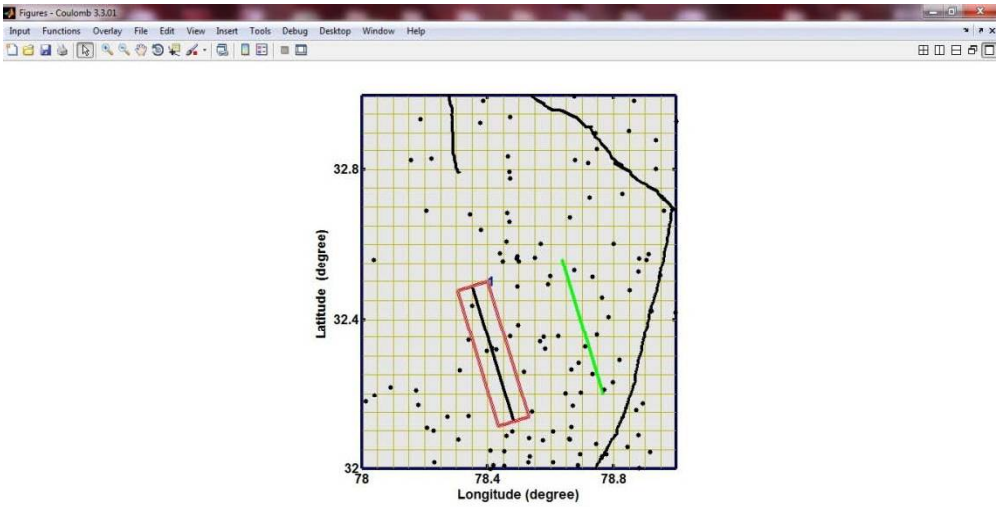

Figure 2.20: The above figure represents the graphic user interface (GUI) for the Coulomb 3.1 application showing the source fault, the epicenter of the source earthquake along with the aftershocks plotted as solid black circle and various other secondary faults as an example.

The next step includes overlying the active fault data and the earthquake data. Here the active fault data in a respective format as a single file is prepared and overlaid it on the prepared base map consisting of the earthquake source. The earthquake hypocenters are plotted on the base map after this under the same routine but with another option of plotting the earthquake hypocenters. *Figure 2.20* figure represents the graphic user interface (GUI) for the Coulomb 3.1 application showing the source fault, the epicenter of the source earthquake along with the aftershocks plotted and various other secondary faults as an example.

In the next step stress estimation is carried out through navigating to the functions option given in the menu bar and selecting the *"calculate the coulomb stress"*option on the targeted fault plane. Here all inputs related to the source parameters of the receiver or targeted fault is provided. These inputs include the Strike, dip and rake of the source fault. The other options such as depth of computation of the coulomb stress and the frictional coefficient are also provided. If anybody wants to change the entire input parameters before computation then it can be changed by utilizing the change

parameters option as shown below.*Figure 2.21* figure represents the graphic user interface (GUI) for the Coulomb 3.1 application showing various options such as depth of computation of the coulomb stress and the frictional coefficient are also needed for the static stress computation.*Figure 2.22* figure represents the graphic user interface (GUI) for the Coulomb 3.1 application showing various options such as strike, dip, rake, type of receiver fault depth of computation and the maximum upto which the static stress is computed as expressed in bars.

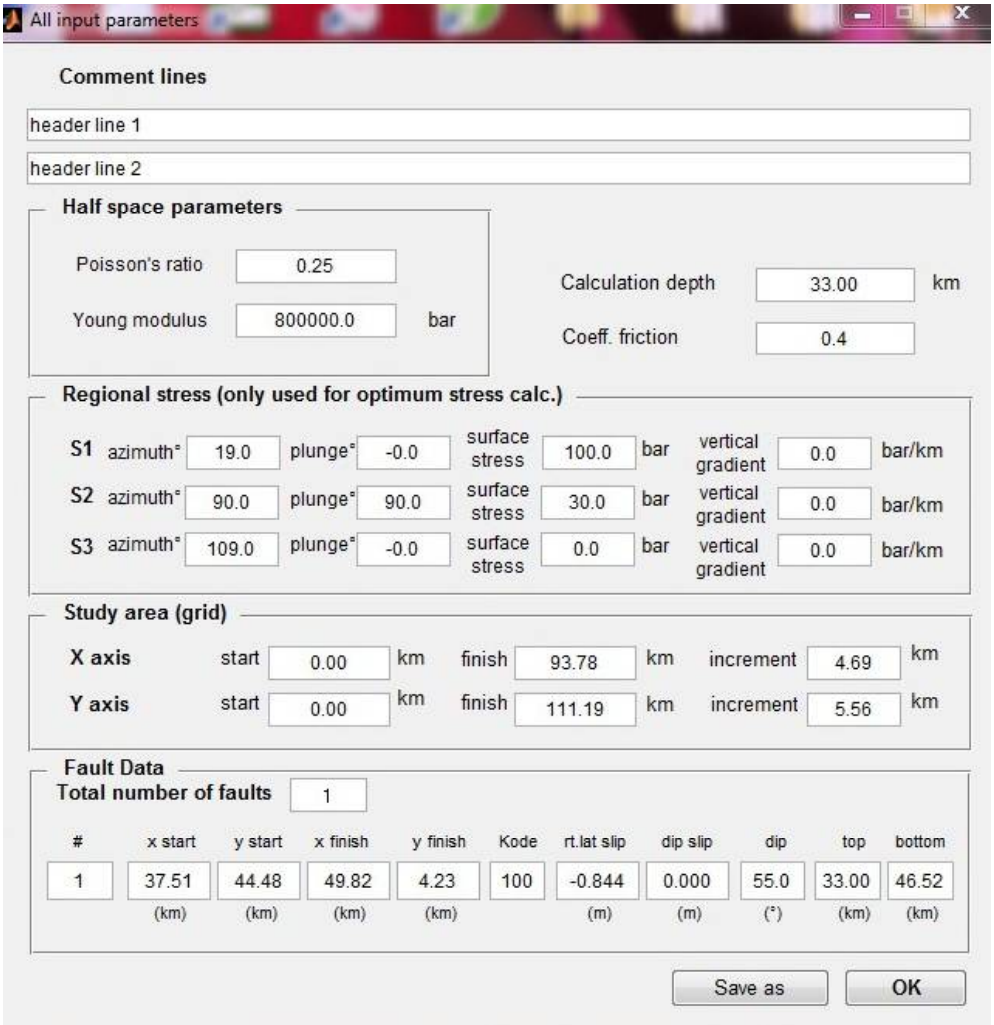

Figure 2.21: The above figure represents the graphic user interface (GUI) for the Coulomb 3.1 application showing various options such as depth of computation of the coulomb stress and the frictional coefficient are also needed for the static stress computation.

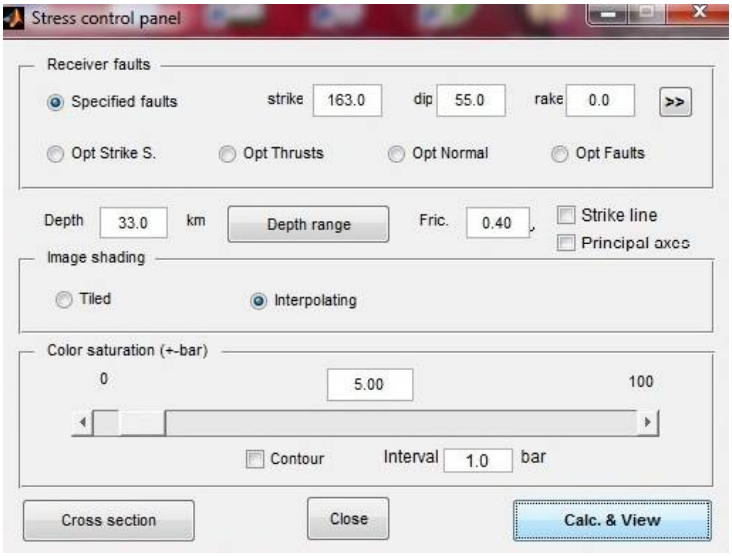

Figure 2.22: The above figure represents the graphic user interface (GUI) for the Coulomb 3.1 application showing various options such as strike, dip, rake, type of receiver fault depth of computation and the maximum upto which the static stress is computed as expressed in bars.

Finally the coulomb stress estimation over a particular receiver fault is estimated and can be visualised below.*Figure 2.23* figure represents the graphic user interface (GUI) for the Coulomb 3.1 application showing the static stress computed as expressed in bars in the study area.

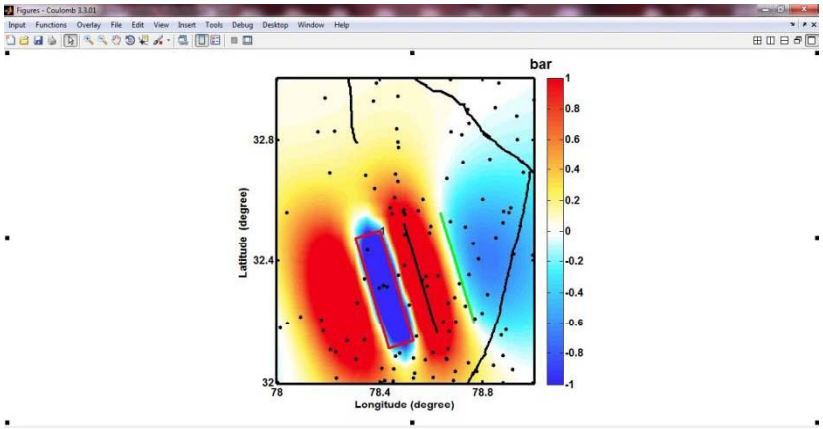

Figure 2.23: The above figure represents the graphic user interface (GUI) for the Coulomb 3.1 application showing the static stress computed as expressed in bars in the study area.

In this way the coulomb static stress change due to three major earthquakes that occurred in the NW Himalaya are estimated applying this Coulomb 3.1 application (Stein, 1999).

2.6. Determination of Frequency Dependency Attenuation Characteristics of Coda Waves

Attenuation is decay in the wave amplitude as the wave propagates through the media. Consequently, its amplitude decay can be attributed to factors like scattering, intrinsic attenuation, geometrical spreading and absorption. As the seismic wave passes through the earth its energy attenuates defining the characteristic of the medium. As established facts suggests that seismic wave attenuation plays a significant role in defining the earthquake source parameter and in seismic hazard assessment. The attenuation characterized and assessed by the inverse of the quality factor. Jin and Aki (1988) states that "the coda quality factor Q_ci.e. the inverse of seismic attenuation factor at frequency of 1 Hz can be used to quantify the seismicity of the concerned area. The Quality factor is calculated using coda method through a single backscattering model. At randomly scattered heterogeneities, the estimation of coda waves has been made as a superimposition of secondary waves through superimposition of backscattering of primary body waves (Aki, 1969; Aki and Chouet, 1975). The coda part of a seismograph comprises of waves that follow numerous paths to reach the recording station, finally to obtain the average attenuation properties of that particular region. Thus, for studying the seismotectonic activities and regional ground structures in the lithosphere the seismic waves attenuation is an important property. The Q_c value obtained in this study is a frequency dependent obtained due to the earthquakes occurring in the NW Himalaya region.

The Q_c values are estimated using the single backscattering model proposed by Aki and Chouet (1975). This model assumes that due to the numerous heterogeneities those are present in the Earth's Crust and Upper Mantle the coda waves are the superposition of backscattered body waves. Origin time, P wave, S wave and Coda window for a seismogram are taken into account. The amplitude of coda waves decreases with lapse time due to

geometrical spreading and attenuation, but it is independent of the earthquake source, path propagation and site amplification (Aki, 1969). The Quality factor generally increases with frequency (Mitchell, 1981) given by the relationship:

$$Q = Q_o (f / f_o) n \quad (2.2)$$

Here, Q_o signify the quality factor at the f_o (usually 1 Hz) reference frequency; f is central frequency and n represent as frequency dependent parameter. This relationship specifies that the seismic wave's attenuation with the increase of distance (from the earthquake source) and time varies with frequencies. Hence, to calculate the attenuation initially it needs to filter all the seismic events at different frequencies using the band pass filter. The single backscattering models (Aki and Chouet, 1975) have been adopted to analyse the coda wave part of Sikkim earthquake aftershocks. According to the single backscattering model, the coda wave amplitude, A (f, t), for a narrow bandwidth signal centred at frequency f and at lapse time t, is described as -

$$A (f, t) = S (f) t^{-a} \exp (-\pi f t / Q_c) \quad (2.3)$$

where, $S(f)$ represents the source function at frequency f and is considered as constant, is the geometrical spreading factor and taken as unity for body waves, and $Q_c$is the quality factor representing the average attenuation characteristics of the medium. Q_C is estimated from the slope (= b) of the equation after rewriting the above equation in the form -

$$\ln [A (f, t) * t] = C - bt \quad (2.4)$$

Hence Q_c is determined from the slope of the graph ln [A (f, t) * t)] vs. t curve, where the slope of the graph is given as -

$$b = \pi f / Q_c \text{ and } C = \ln S(f) \quad (2.5)$$

In the present context of the seismic attenuation study carried out in the NW Himalaya the seismic waveform data of 132 hypocenters with an epicentral distance within the 240 km within the seismic array. The next step involves the band passing of these waveform data utilizing an eight pole Butterworth filter. The frequency bands are at 1.5 ± 0.5 Hz, 3 ± 1 Hz, 5 ± 1 Hz, 7 ± 1 Hz, 9 ± 1 Hz, 12 ± 1 Hz, 16 ± 1 Hz, 20 ± 2 Hz, 24 ± 2 Hz, and 28 ± 2 Hz. In the next step, the root mean squared amplitudes of these ten filtered seismograms are computed at an interval of 0.5s with moving time windows of length t ± 2 s for the first frequency band and t ± 1 s for the next nine frequency bands. Q_C is then estimated applying a least square regression technique for six starting lapse time windows of length LT= 10, 20, 30, 40, 50, and 60 s from the S-wave onset, having window lengths of WL= 10, 20, 30, 40, and 50 s. In this way the Frequency dependent seismic attenuation characteristic of the NW Himalaya has been calculated utilizing the coda normalization technique.

2.7. Gravity Anomaly and Lithospheric Structure for the NW Himalaya

The gravity anomaly map of the NW Himalaya region is studied in order to understand the seismotectonics which will provide a major tectonic implication along with seismological study. The Isotactic gravity anomalies and effective elastic thickness (EET) of lithosphere are assessed from coherence analysis between Bouguer anomaly and topography. The Bouguer gravity anomaly map is then correlated and the parts of gravity high and low are obtained and correlated with the major tectonic provinces of the region. The effective elastic thickness (EET) is determined using the coherence analysis and the cut off frequency as obtained from it. And after applying the cut off frequency the Isostatic residual anomaly is obtained. Next, the regional modelling is carried out by fixing the Moho depth and density for the region and various tectonic implications has been derived.